

The Dynamical Power Corrections in hadronic B decays

Tsung-Wen Yeh*

Department of Nature Science Education, National Taichung Teachers College, Taichung 403, Taiwan

We calculate the subleading power suppressed corrections arising from the three parton Fock state of the final state pseudoscalar light mesons in hadronic B decays. The three parton corrections are evaluated up to $O(\alpha_s^2)$ and $O(1/m_b)$. Our result shows that the three parton contributions are important in understanding of penguin dominant processes. The sign pattern of the predicted CP asymmetries for $B \rightarrow \pi K, \pi\pi$ decays is the same with that of experimental data.

PACS numbers: 12.38.Bx, 14.40.-n

Recent years, many rare hadronic decays of B mesons are accessible. They are helpful for studies of CP violation and explorations of new physics beyond the standard model. To understand the physics related to rare processes, it requires a precisely theoretical formalism for estimating the three body matrix elements of the electroweak effective Hamiltonian. The QCD factorization [1], which generalizes the naive factorization, provides such an basis. In the heavy quark mass limit, the QCD factorization demonstrates that the three body matrix element of the effective Hamiltonian could be expressed in terms of a factorization form, in which the short and long distance strong interactions are written as separately incoherent functions. Beyond the large mass limit, the validity of factorization properties of the matrix elements could be questionable due to subleading power suppressed corrections [1]. In phenomenology, the power suppressed corrections could not be negligible for accommodating experimental data [2, 3]. So far, there still lacks a systematic method for power suppressed corrections. In order to explore the relevant mechanisms, it is interesting to find out as possible as many kinds of power suppressed corrections.

The power suppressed corrections may come from different sources, such as, the mismatch between the total spin of the Fock state and that of its composed meson [8], the higher Fock states [8], the final state interactions [5, 6, 7], the soft gluon corrections [1], the annihilation corrections [1], the spectator corrections [1], the IR renormalon corrections [9]. In this work, we would like to investigate the chirally enhanced power suppressed corrections resulting from three parton $q\bar{q}g$ Fock state of final states in hadronic decays of B mesons into two pseudoscalar mesons. The gluons among the corrections are collinear partons of relevant mesons. The corrections arise from quark gluon interaction terms in the QCD Lagrangian, and are named as dynamical power corrections to reflect its dynamical nature. We employed the convention of [4] for definitions of relevant functions.

The chirally enhanced power suppressed corrections are important for understanding of penguin dominant processes and extraction of CP violation phases. In previous studies [1, 4], the chirally enhanced power suppressed corrections only include contributions from twist-3 two parton distribution amplitudes (DAs), the pseudoscalar and pseudotensor DAs. The contributions associated with the twist-3 three parton DA are completely ignored by assuming that they are suppressed by a small normalization factor of the DA. To complete studies of chirally enhanced power suppressed corrections at twist-3 order, and to see how the above approximation is good enough or not, we intend to investigate the contributions associated with the twist-3 three parton DA.

Up to one loop radiative corrections, the investigated three parton corrections are of twist-3 order, *i.e.*, corrections being suppressed by $1/m_b$, with m_b being the b quark mass. At tree level, the $q\bar{q}g$ Fock state of M_2 in the $B \rightarrow M_1 M_2$ decays contributes through the $-2(S-P) \otimes (S+P)$ operator. Its result as combined with the other two parton contributions appears as

$$\langle M_1 M_2 | Q_{(S-P)(S+P)} | B \rangle = c_Q (1 + A_{M_2}^{G_3}) r_\chi^{M_2} A_{M_1 M_2}, \quad (1)$$

where $c_Q = 1$ for Q_6 and $c_Q = 3e_Q/2$ for Q_8 . $A_{M_2}^{G_3}$ represents the three parton corrections from the tree level diagrams as depicted in Fig. 1(a) and 1(b)

$$A_{M_2}^{G_3} = 2 \int [d\alpha] \delta(1 - \Sigma\alpha) \frac{T_{M_2}(\alpha_{\bar{q}_2}, \alpha_{q_1}, \alpha_g)}{\alpha_{q_1} \alpha_g}, \quad (2)$$

where $A_{M_1 M_2} = i(M_B^2 - m_{M_2}^2) F_0^{B \rightarrow M_1}(m_{M_2}^2) f_{M_2}$, and $r_\chi^{M_2} = 2m_{M_2}^2 / [\bar{m}_b(\bar{m}_{q_1} + \bar{m}_{q_2})]$. The integral measure $[d\alpha]$ is an abstract notation for $d\alpha_{\bar{q}_2} d\alpha_{q_1} d\alpha_g$. The three parton distribution amplitude $T_{M_2}(\alpha_{\bar{q}_2}, \alpha_{q_1}, \alpha_g)$ parameterizes the matrix element $\langle M_2 | \bar{q}_1(z) \sigma_{\mu\nu} \gamma_5 g G_{\alpha\beta}(y) q_2(x) | 0 \rangle$ and has a parameterization form $T(\alpha_{\bar{q}_2}, \alpha_{q_1}, \alpha_g) = 360\eta \alpha_{\bar{q}_2} \alpha_{q_1} \alpha_g^2 (1 +$

*Electronic address: twyeh@ms3.ntctc.edu.tw

$\omega/2(7\alpha_g - 3)$). For most pseudoscalar mesons, such as π, K and η , $\eta = 0.015$ and $\omega = -3$. It results in that $A_{M_2}^{G_3} = 0.585$. The three parton effects then enhance 50% of the twist-3 two parton contribution. The diagrams as depicted in Fig. 1(c) and (d) are of at least twist-4 and would vanish due to the G-parity. Their effects will not be considered further in this work. The large effect of three parton corrections is due to the associated partonic amplitude in Eq. (2), which behaves as $1/(\alpha_{q_1}\alpha_g)$. The evaluation of diagrams in Fig. 1 depends on the gauge choice for gluon fields. The light-cone gauge and the covariant gauge have been employed for calculations. An explicit evaluation shows that the result is gauge independent. To facilitate calculations for one loop corrections, we employed the covariant gauge for both collinear and radiative virtual gluons.

The associated short distance coefficient a_i , for $i = 6, 8$, including one loop radiative corrections from the three parton contributions, is expressed as

$$a_i = C_i + \frac{C_{i-1}}{N_C}(1 + V_{M_2,3}\frac{C_F\alpha_s}{4\pi}) + \frac{C_F\alpha_s}{4\pi N_C}P_{M_2,3}, \quad (3)$$

where $V_{M_2,3}$ and $P_{M_2,3}$ denote contributions from vertex and penguin diagrams, respectively. The additional quark-gluon vertex are inserted into the vertex and penguin diagrams in all possible ways. There are totally 32 vertex diagrams similar to that one depicted in Fig. 2(a). Only those diagrams with inserted vertices exterior to the radiative loop can contribute at twist-3 order. The others are of twist-4, $O(1/m_b^2)$ or higher. The cross vertex in the diagram of Fig. 2(a) denotes a vertex $i\gamma_\nu$, which comes from a collinear expansion of the quark propagator in the diagram. As an example, we take the evaluation of Fig. 2(a) to introduce the collinear expansion. The amplitude for the Feynman diagram of Fig. 2(a) is proportional to the convolution integration over the loop parton momenta l_q and l_g

$$\int \frac{d^4 l_q}{(2\pi)^4} \int \frac{d^4 l_g}{(2\pi)^4} \text{Tr}[H_\mu(l_q, l_g)\phi^\mu(l_q, l_g)], \quad (4)$$

where $H_\mu(l_q, l_g)$ represents a partonic amplitude as depicted in the diagram, and $\phi^\mu(l_q, l_g)$ denotes the amplitude with which the $q\bar{q}g$ state composes into the meson M_2

$$\phi^\mu(l_q, l_g) = \int d^4 x \int d^4 y e^{il_{q_1} \cdot x} e^{il_g \cdot y} \langle M_2 | \bar{q}_1(x) (-gA^\mu(y)) q_2(0) | 0 \rangle. \quad (5)$$

The trace is taken over fermion and color indices. By scale analysis, we found that the dominant contributions arise from collinear region in which both l_q and l_g are collinear to their external meson. Then, it is followed by a Taylor expansion of $H_\mu(l_{q_1}, l_g)$ with respect to $\hat{l}_{q_1} = \alpha_{q_1} q$ and $\hat{l}_g = \alpha_g q$ as

$$H_\mu(l_{q_1}, l_g) = H_\mu(\hat{l}_{q_1}, \hat{l}_g) + \frac{dH_\mu}{dk^\nu} \Big|_{k=\hat{k}} (k - \hat{k})^\nu + \dots, \quad (6)$$

where $k = l_q + l_g$ in the second term of rhs of the above equation. The derivative of $H_\mu(k)$ over momentum k is applied on propagators containing the momentum k . The dominant contributions arise from the cases in which the derivative is applied on the quark propagator exterior to the radiative loop. In covariant gauge, the first term in Eq. (6) is related to gauge phase factors and the second term is relevant to three parton contributions. The sophisticated reader may notice that there may arise end point divergence from the denominator of the second term. This divergence will be cancelled out after combining the denominator and numerator of the amplitude. To complete the calculation, standard decomposition procedures for fermion and color indices are required.

The calculations of 32 vertex diagrams are collected in the function $V_{M_2,3}^{G_3}$ of $V_{M_2,3} = -6 + V_{M_2,3}^{G_3}$, which is expressed as

$$V_{M_2}^{G_3} = -6 \int [d\alpha] T_{M_2}(\alpha_{\bar{q}_2}, \alpha_{q_1}, \alpha_g) \frac{g(\alpha_{\bar{q}_2})}{\alpha_{q_1} \alpha_g} \quad (7)$$

where

$$g(\alpha) = 2\left(\frac{\ln \bar{\alpha}}{\alpha} - \frac{\ln \alpha}{\bar{\alpha}}\right) + (\text{Li}_2(1 - \frac{1}{\alpha}) - \text{Li}_2(1 - \frac{1}{\bar{\alpha}})) + 2(\ln \bar{\alpha} - \ln \alpha) + 2\left(\frac{\alpha}{\bar{\alpha}} \ln \alpha - \frac{\bar{\alpha}}{\alpha} \ln \bar{\alpha}\right). \quad (8)$$

With corrections from the three parton Fock state, the penguin corrections $P_{M_2,3} = P_{M_2,3}^2 + P_{M_2,3}^{G_3}$, with $P_{M_2,3}^2$ and $P_{M_2,3}^{G_3}$ being contributions from two [4] and three parton twist-3 DAs. The function $P_{M_2,3}^{G_3}$ collecting calculations for 42 diagrams similar to Fig. 2(b) can be written as

$$P_{M_2,3}^{(P)G_3}(\mu) = \left[C_1 \left[2A_{M_2}^{G_3}(\ln(m_b/\mu) - \frac{2}{3}) + G_{M_2}^{G_3}(s_c) \right] + C_3 \left[4A_{M_2}^{G_3}(\ln(m_b/\mu) - \frac{2}{3}) + G_{M_2}^{G_3}(0) + G_{M_2}^{G_3}(1) \right] \right. \\ \left. + (C_4 + C_6) \left[2n_f A_{M_2}^{G_3}(\ln(m_b/\mu) - \frac{1}{3}) + (n_f - 2)G_{M_2}^{G_3}(0) + G_{M_2}^{G_3}(s_c) + G_{M_2}^{G_3}(1) \right] \right], \quad (9)$$

where

$$G_{M_2}^{G_3}(s) = -3 \int [d\alpha] T_{M_2}(\alpha_{\bar{q}_2}, \alpha_{q_1}, \alpha_g) \frac{G(s, 1 - \alpha_{\bar{q}_2})}{\alpha_{q_1} \alpha_g} \quad (10)$$

and $G(s, x)$ is the penguin function. The factorization scale dependence of a_i is implied and the scale has been chosen to be m_b .

For annihilation diagrams, the three parton contributions participate through $-2(S - P) \otimes (S + P)$ operators. Their effects are to modify the $A_3^{i(f)}$ functions into $A_3^{i(f)} = A_{3,2}^{i(f)} + A_{3,G_3}^{i(f)}$. $A_{3,2}^{i(f)}$ and $A_{3,G_3}^{i(f)}$ denote the two and three parton contributions, respectively. A_3^i is much smaller than A_3^f and can be neglected. Collecting calculations for 48 annihilation diagrams, one then obtains

$$\begin{aligned} A_{3,G_3}^f &= 6\pi\alpha_s r_\chi^{M_i} \int_0^1 dx \int_0^1 dy \left[\delta_{M_1}^{M_i} \delta(y - \alpha_{\bar{q}_2}) \phi_{M_2}(x) + \delta_{M_2}^{M_i} \delta(\bar{x} - \alpha_{\bar{q}_2}) \phi_{M_1}(y) \right] \int [d\alpha] \frac{T_{M_i}(\alpha_{\bar{q}_2}, \alpha_{q_1}, \alpha_g)}{\bar{x} y \alpha_{q_1} \alpha_g} \\ &\approx \left(\frac{9}{80} \right) \times 6\pi\alpha_s (r_\chi^{M_1} + r_\chi^{M_2}). \end{aligned} \quad (11)$$

It is noted that A_{3,G_3} is free from end-point divergence. Compared to $A_{3,2}^f$, A_{3,G_3}^f is only 1.5% of $A_{3,2}^f$, which has a large numerical value due to its end point divergences. The endpoint divergence has a large uncertainty in a phase ϕ_A ranging between 0 and 2π . Under assumption of an 100% uncertainty in ϕ_A [4], A_3^f is almost equal to $A_{3,2}^f$ and the contribution from twist-3 three parton DAs can be neglected. At twist-3 order, there are no chirally enhanced three parton contributions associated with $(V - A) \otimes (V \pm A)$ operators. This is due to the spin structure of $(V - A) \otimes (V \pm A)$ operators, and/or pair cancellations between diagrams.

The numerical values of relevant functions are $A_{M_2}^{G_3} = 0.585$, $V_{M_2}^{G_3} = 2.363$, $P_{M_2,3}^{G_3}(m_b) = -0.827 - 0.388i$ and $A_{3,G_3}^f(1.45\text{GeV}) = 1.049$, in which the input parameters listed in the Table 1 of [4] have been used. According to the notation of [4], the decay amplitudes are expressed in terms of α_i^p and β_i^p , for $i = 1, \dots, 4$ and $p = u, c$, and $A_{M_1 M_2}$ with $M_1 M_2 = \pi K, \pi\pi$. The definitions of α_i^p and β_i^p refer to [4]. For comparison, the values of $\alpha_i^p(\pi\pi)$ and $\beta_i^p(\pi\pi)$ at scale $\mu = m_b$ are evaluated in Table I. The relevant Wilson coefficients $C_i(\mu)$, $i = 1, \dots, 10$, are evaluated in Table II by employing the NLO formula [10, 11, 12, 13]. It is noted that the values in Table II are in agreement with [1, 13]. In Table I, we list values of α_4^c with or without including the three parton contributions (the numbers in the parenthesis). It is shown that α_4^c are enhanced by 15% due to three parton effects. It is also noted that the evaluated values of the two parton parts of α_i^p and β_i^p are in agreement with [4]. However, the 20% differences in values of α_4^p and β_3^p between our evaluation and that of [4] leads to large different predictions for branching ratios and CP asymmetries (see below explanations).

We now apply the above calculations to make predictions for CP-averaged branching ratios, and for direct CP asymmetries, under " \bar{B} minus B " convention, for $B \rightarrow \pi K$ and $B \rightarrow \pi\pi$ decays. The predicted CP-averaged branching ratios and direct CP asymmetries are listed in Table III. The most recent results from BaBar, Belle, CLEO experiments and world average [14] are also shown. For comparison, similar results quoted from [4] are also listed.

For penguin dominant $B \rightarrow \pi K$ processes, it is shown that the three parton effects are significant in the predicted branching ratios. The predicted branching ratio of process $B^- \rightarrow \pi^- \bar{K}^0$ is increased close to new experimental data. It is noted that the two parton predictions (the column I) are lower than the experimental data. From Table III, it is noted that our two parton predictions for branching ratios of $B^- \rightarrow \pi^0 \bar{K}^-$, $B^- \rightarrow \pi^0 K^-$, $\bar{B}^0 \rightarrow \pi^+ K^-$ are smaller than those predictions of [4] (the third column) by a factor $1.6 \sim 1.7$. This factor may come from the difference between numerical values of α_4^p evaluated in this work and that by [4]. For tree dominant $B \rightarrow \pi\pi$ processes, twist-3 three parton contributions have small effects as expected.

Due to large uncertainties in experimental data for CP asymmetries of $B \rightarrow \pi K, \pi\pi$ decays, it is still difficult to reach a solid conclusion for theoretical predictions. From Table III, it is noted that our predictions for A_{CP} have the same sign pattern of experimental data, while the predictions from [4] have a different sign pattern. This solves the problem of QCD factorization in predictions of CP asymmetry. The reason could be expressed by our use of a complete NLO formula of Wilson coefficient C_i without taking approximations as the treatment in [1], since the CP asymmetry is sensitive to small differences between predictions for $Br(\bar{B} \rightarrow \bar{f})$ and $Br(B \rightarrow f)$, and the phase γ is always accompanied by Wilson coefficients. The details about this point will be given elsewhere.

In this work, we have employed the collinear expansion method to evaluate three parton contributions for decays of B mesons into two pseudoscalar mesons up to $O(\alpha_s^2)$ and $O(1/m_b)$. Our analysis showed that the three parton contributions enhance the chirally enhanced power suppressed corrections by 50% and 15% from tree and one loop corrections, respectively. The result is then applied to make predictions for CP-averaged branching ratios and direct CP asymmetries for processes $B \rightarrow \pi K, \pi\pi$. We also solve the sign pattern problem of QCD factorization in predictions of CP asymmetry.

Acknowledgements The author appreciates partial financial support from the National Science Council under grand numbers NSC-93-2112-M-142-001 and NSC-94-2112-M-142-001 .

-
- [1] M. Beneke, G. Buchalla, M. Neubert and C. T. Sachrajda, Nucl. Phys. B **606**, 245 (2001) [arXiv:hep-ph/0104110].
 - [2] N. de Groot, W. N. Cottingham and I. B. Whittingham, Phys. Rev. D **68**, 113005 (2003) [arXiv:hep-ph/0308269].
 - [3] T. N. Pham and G. Zhu, Phys. Rev. D **69**, 114016 (2004) [arXiv:hep-ph/0403213].
 - [4] M. Beneke and M. Neubert, Nucl. Phys. B **675**, 333 (2003) [arXiv:hep-ph/0308039].
 - [5] Z. z. L. Xing, Phys. Lett. B **493**, 301 (2000) [arXiv:hep-ph/0007136].
 - [6] P. Zenczykowski, Phys. Rev. D **63**, 014016 (2001) [arXiv:hep-ph/0009054].
 - [7] K. Terasaki, Int. J. Theor. Phys. Group Theor. Nonlin. Opt. **8**, 55 (2002) [arXiv:hep-ph/0011358].
 - [8] P. Ball, JHEP **9901**, 010 (1999) [arXiv:hep-ph/9812375].
 - [9] M. Neubert and B. D. Pecjak, JHEP **0202**, 028 (2002) [arXiv:hep-ph/0202128].
 - [10] A. J. Buras, M. Jamin and M. E. Lautenbacher, Nucl. Phys. B **400**, 75 (1993) [arXiv:hep-ph/9211321].
 - [11] M. Ciuchini, E. Franco, G. Martinelli and L. Reina, Phys. Lett. B **301**, 263 (1993) [arXiv:hep-ph/9212203].
 - [12] M. Ciuchini, E. Franco, G. Martinelli and L. Reina, Nucl. Phys. B **415**, 403 (1994) [arXiv:hep-ph/9304257].
 - [13] G. Buchalla, A. J. Buras and M. E. Lautenbacher, Rev. Mod. Phys. **68**, 1125 (1996) [arXiv:hep-ph/9512380].
 - [14] H. F. A. Group, arXiv:hep-ex/0505100.

$\alpha_i(\pi\pi)$		[4]	$\beta_i(\pi\pi)$		[4]
α_1	0.99	0.99	β_1	0.026	0.025
α_2	0.23	0.20	$-\beta_2$	0.008	0.010
$-\alpha_3$	0.01	-	$-\beta_3$	0.014	0.009
$-\alpha_4^c$	0.095(0.085)	0.102	$-\beta_4$	0.003	-

TABLE I: Amplitude factors for $B \rightarrow \pi\pi$ decays. The scale is at m_b .

C_i	$\sqrt{\lambda_h m_b}/2$	$\sqrt{\lambda_h m_b}$	$\sqrt{2\lambda_h m_b}$	$m_b/2$	m_b	$2m_b$
C_1	1.251	1.190	1.146	1.144	1.086	1.047
$-C_2$	0.468	0.373	0.301	0.297	0.191	0.113
C_3	350	268	212	209	136	88
$-C_4$	761	615	510	504	354	246
C_5	120	124	118	118	98.4	76.6
$-C_6$	1157	862	673	662	427	279
$-C_7$	0.489	0.984	1.000	0.989	0.159	-1.384
C_8	14.2	10.3	7.82	7.68	4.81	3.086
$-C_9$	111	107	103	103	97.6	93.1
C_{10}	41.6	33.5	28.1	27.7	19.4	12.9

TABLE II: The Wilson coefficients $C_i(\mu)$, $i = 1, \dots, 10$ are evaluated at scales $\mu = \sqrt{\lambda_h m_b}/2, \sqrt{\lambda_h m_b}, \sqrt{\lambda_h 2m_b}, m_b/2, m_b, 2m_b$, with $\lambda_h = 0.5 \text{ GeV}$. The values of C_{3-10} are in units of 10^{-4} .

Br	I	II	[4]	BaBar	Belle	CLEO	average
$B^- \rightarrow \pi^- K^0$	$11.4^{+0.2}_{-0.1}$	$21.9^{+0.2}_{-0.3}$	$19.3^{+1.9}_{-1.9}$	$26.0 \pm 1.3 \pm 1.0$	$22.0 \pm 1.9 \pm 1.1$	$18.8^{+3.7+2.1}_{-3.3-1.8}$	24.1 ± 1.3
$B^- \rightarrow \pi^0 K^-$	$6.9^{+1.0}_{-0.9}$	$17.9^{+1.6}_{-1.4}$	$11.1^{+1.8}_{-1.7}$	$12.0 \pm 0.7 \pm 0.6$	$12.0 \pm 1.3^{+1.3}_{-0.9}$	$12.9^{+2.4+1.2}_{-2.2-1.1}$	12.1 ± 0.8
$\bar{B}^0 \rightarrow \pi^+ K^-$	$10.0^{+1.4}_{-1.2}$	$18.6^{+1.8}_{-1.6}$	$16.3^{+2.6}_{-1.7}$	$17.9 \pm 0.9 \pm 0.7$	$18.5 \pm 1.0 \pm 0.7$	$18.0^{+2.3+1.2}_{-2.1-0.9}$	18.2 ± 0.8
$\bar{B}^0 \rightarrow \pi^0 \bar{K}^0$	$6.7^{+1.7}_{-1.6}$	$16.0^{+2.8}_{-2.5}$	$7.0^{+0.7}_{-0.7}$	$11.4 \pm 0.9 \pm 0.6$	$11.7 \pm 2.3^{+1.2}_{-1.3}$	$12.8^{+4.0+1.7}_{-3.3-1.4}$	11.5 ± 1.0
$\bar{B}^0 \rightarrow \pi^+ \pi^-$	$7.9^{+0.9}_{-1.1}$	$8.1^{+1.6}_{-1.7}$	$8.9^{+4.0}_{-3.4}$	$4.7 \pm 0.6 \pm 0.2$	$4.4 \pm 0.5 \pm 0.3$	$4.5^{+1.4+0.5}_{-1.2-0.4}$	4.5 ± 0.4
$B^- \rightarrow \pi^- \pi^0$	$4.6^{+0.6}_{-0.3}$	$4.5^{+0.8}_{-0.6}$	$6.0^{+3.0}_{-2.4}$	$5.8 \pm 0.6 \pm 0.4$	$5.0 \pm 1.2 \pm 0.5$	$4.6^{+1.8+0.6}_{-1.6-0.7}$	5.5 ± 0.6
$\bar{B}^0 \rightarrow \pi^0 \pi^0$	$0.1^{+0.1}_{-0.5}$	$0.2^{+0.2}_{-0.1}$	$0.3^{+0.2}_{-0.2}$	$1.17 \pm 0.32 \pm 0.10$	$2.3^{+0.4+0.2}_{-0.5-0.3}$	< 4.4	1.45 ± 0.29
A_{CP}	I	II	[4]	BaBar	Belle	CLEO	average
$B^- \rightarrow \pi^- K^0$	0.05 ± 0.01	$0.5^{+0.04}_{-0.1}$	$0.9^{+0.2}_{-0.3}$	$8.7 \pm 4.6 \pm 1.0$	$-5.0 \pm 5.0 \pm 1.0$	$-18 \pm 24 \pm 2$	2.0 ± 3.4
$B^- \rightarrow \pi^0 K^-$	$-20.6^{+1.4}_{-0.9}$	$-6.4^{+0.8}_{-0.0}$	$7.1^{+1.7}_{-1.8}$	$-6 \pm 6 \pm 1$	$-4 \pm 5 \pm 2$	$29 \pm 23 \pm 2$	-4 ± 4
$\bar{B}^0 \rightarrow \pi^+ K^-$	$-18.5^{+1.4}_{-0.0}$	$-6.4^{+0.7}_{-0.0}$	$4.5^{+1.1}_{-1.1}$	$-13.3 \pm 3.0 \pm 0.9$	$-10.1 \pm 2.5 \pm 0.5$	$-4 \pm 16 \pm 2$	-10.9 ± 1.9
$\bar{B}^0 \rightarrow \pi^0 \bar{K}^0$	$-38.6^{+6.1}_{-2.6}$	$-11.1^{+0.4}_{-0.1}$	$-3.3^{+1.0}_{-0.8}$	$-3 \pm 36 \pm 11$	$-16 \pm 29 \pm 5$		-11 ± 23
$\bar{B}^0 \rightarrow \pi^+ \pi^-$	$16.5^{+3.7}_{-4.5}$	$9.2^{+3.3}_{-2.8}$	$-6.5^{+2.1}_{-2.1}$	$9 \pm 15 \pm 4$	$56 \pm 12 \pm 6$		37 ± 10
$B^- \rightarrow \pi^- \pi^0$	$37.6^{+4.1}_{-9.8}$	$35^{+6.7}_{-10.4}$	$-0.02^{+0.01}_{-0.01}$	$1 \pm 10 \pm 2$	$2 \pm 10 \pm 1$		2 ± 7
$\bar{B}^0 \rightarrow \pi^0 \pi^0$	$17.5^{+55.8}_{-22.9}$	$1.2^{+29.3}_{-9.2}$	$45.1^{+18.4}_{-12.8}$	$12 \pm 56 \pm 6$	$44^{+53}_{-52} \pm 17$		28^{+40}_{-59}

TABLE III: The column I and II are predictions without and with including three parton corrections, respectively. The branching ratios are in units of 10^{-6} and the CP asymmetries in units of 10^{-2} . The errors for predictions in column I and II correspond to $\gamma = 70 \pm 20$. The combination of uncertainties in V_{ub}, V_{cb} and γ refers to the errors in the third column.

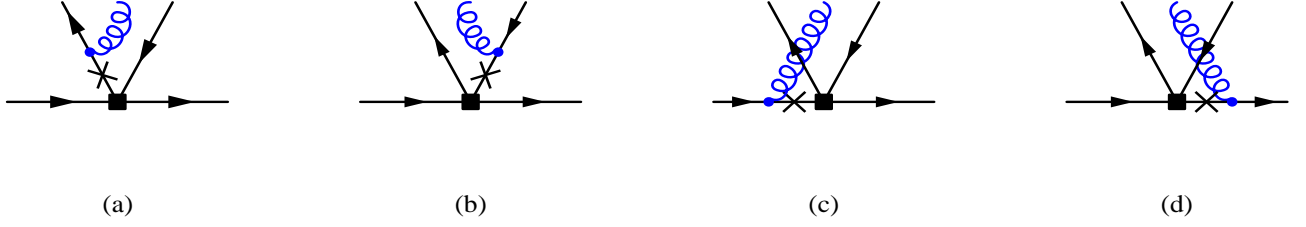


FIG. 1: The one gluon insertion diagrams for $B \rightarrow P_1 P_2$. The square symbol represents the vertex of weak interactions. The explanation of the cross vertex refers to the text.

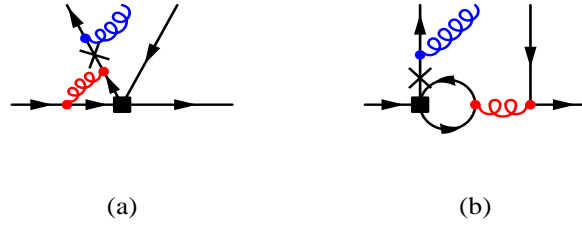


FIG. 2: The vertex and penguin diagrams with one gluon insertion. The square symbol represents the vertex of weak interactions. The explanation of the cross vertex refers to the text.